

Local-feature-based similarity measure for stochastic resonance in visual perception of spatially structured images

Agnès Delahaies,¹ David Rousseau,^{2,*} Jean-Baptiste Fasquel,¹ and François Chapeau-Blondeau¹

¹Laboratoire d'Ingénierie des Systèmes Automatisés (LISA), Université d'Angers, 62 avenue Notre Dame du Lac, 49000 Angers, France

²Université de Lyon, CREATIS; CNRS, UMR5220; INSERM, U1044; Université Lyon 1; INSA-Lyon, 69621 Villeurbanne, France

*Corresponding author: david.rousseau@univ-lyon1.fr

Received January 10, 2012; accepted March 21, 2012;
posted April 9, 2012 (Doc. ID 161168); published June 4, 2012

For images, stochastic resonance or useful-noise effects have previously been assessed with low-level pixel-based information measures. Such measures are not sensitive to coherent spatial structures usually existing in images. As a result, we show that such measures are not sufficient to properly account for stochastic resonance occurring in visual perception. We introduce higher-level similarity measures, inspired from visual perception, and based on local feature descriptors of scale invariant feature transform (SIFT) type. We demonstrate that such SIFT-based measures allow for an assessment of stochastic resonance that matches the visual perception of images with spatial structures. Constructive action of noise is registered in this way with both additive noise and multiplicative speckle noise. Speckle noise, with its grainy appearance, is particularly prone to introducing spurious spatial structures in images, and the stochastic resonance visually perceived and quantitatively assessed with SIFT-based measures is specially examined in this context. © 2012 Optical Society of America

OCIS codes: 000.2690, 100.5010, 030.6140, 030.4280, 100.2000, 120.6150.

1. INTRODUCTION

It is now an established fact (see [1] for a recent survey) that the presence of a nonzero level of noise in nonlinear systems can sometimes provide a benefit to the information processing by these systems. Introduced in physics in the 1980s under the common designation of stochastic resonance, constructive action of noise has since been uncovered in many other domains connected to information sciences, including photonics [2–8], electronics, or neurosciences (see [1] for a review). Purposeful injection of noise at a controlled level predictable by theoretical analysis of stochastic resonance is useful in constrained situations where a nonlinear system in charge of information processing is natively positioned in an unfavorable manner to convey this information. Thanks to theoretical analysis and physical experiment, the understanding of the various mechanisms by which stochastic resonance can operate has greatly progressed over the last years [1]. However, a central question remaining is whether our neural system, which performs information processing in the presence of noise and nonlinearities, actually uses stochastic resonance *in vivo*. This question can be considered at different levels with isolated neurons, with associations of neurons up to the maximal integration level with the psychosensorial experiment. In this article, we work at the level of the psychosensorial experiment. We revisit a recent demonstration of visual perception of stochastic resonance, and we demonstrate that the mechanism at work in those experiments needs to be further analyzed to understand the influence of spatial structures in the constructive action of the noise in imaging systems.

2. VISUAL PERCEPTION OF STOCHASTIC RESONANCE

We consider, as situation of reference, the stochastic resonance effect studied in [9,10], where an initial input binary image \mathbf{x} is corrupted with an additive centered Gaussian white noise \mathbf{n} and transmitted by a two-level quantizer with threshold θ as

$$\mathbf{y} = g(\mathbf{x} + \mathbf{n}), \quad (1)$$

and

$$g(x) = \begin{cases} 0 & \text{for } x \leq \theta \\ 1 & \text{for } x > \theta. \end{cases} \quad (2)$$

Figures 1(a)–1(d) show a visual effect of the nonlinear transmission aided by noise as in [7] when the standard deviation of the noise root mean square (rms) amplitude is raised.

To complement the visual perception involved in Fig. 1, we assess the nonlinear information transmission between images \mathbf{x} and \mathbf{y} with objective quantitative measures. The nonlinearity $g(\cdot)$ of Eq. (2) operates a pixel to pixel process. Input image \mathbf{x} and output images \mathbf{y} are noisy images with object and background. Both regions' object and background are contrasted by the difference in their statistical properties. A natural proposal is therefore to begin with low-level pixel-based information measures. We turn to three measures of similarity, also used in [10], under the form of the normalized input–output cross-covariance

$$C(\mathbf{x}, \mathbf{y}) = \frac{\langle xy \rangle - \langle x \rangle \langle y \rangle}{\sqrt{\langle x^2 \rangle - \langle x \rangle^2} \sqrt{\langle y^2 \rangle - \langle y \rangle^2}}, \quad (3)$$

and the structural similarity index (SSIM) introduced by [11]

$$S(\mathbf{x}, \mathbf{y}) = \frac{4(\langle xy \rangle - \langle x \rangle \langle y \rangle) \langle x \rangle \langle y \rangle}{(\langle x^2 \rangle - \langle x \rangle^2 + \langle y^2 \rangle - \langle y \rangle^2)(\langle x \rangle^2 + \langle y \rangle^2)}, \quad (4)$$

where $\langle \cdot \rangle$ is an ensemble average over the pixels of the images. As a complement to C , and S , we add a third measure of similarity with the Shannon mutual information

$$I(\mathbf{x}, \mathbf{y}) = H(\mathbf{y}) - H(\mathbf{y}|\mathbf{x}), \quad (5)$$

where $H(\cdot)$ is the standard Shannon entropy

$$H(\mathbf{y}) = \int_y -dy p_y(y) \log_2[p_y(y)], \quad (6)$$

and

$$H(\mathbf{y}|\mathbf{x}) = \int_x dx p_x(x) \int_y -dy p_{y|x}(y) \log_2[p_{y|x}(y)] \quad (7)$$

with the conditional probability density given by $p_{y|x}(y)dy = \Pr\{\mathbf{y} \in [y, y + dy]|\mathbf{x} = x\}$, and the marginal density $p_y(y) = \int_x dx p_x(x)p_{y|x}(y)$. For the input-output binary images \mathbf{x} and \mathbf{y} , it is possible to derive analytical expressions for the similarity measures C, S, I of Eqs. (3), (4), and (5). This gives

$$C(\mathbf{x}, \mathbf{y}) = \frac{p_1(p_{11} - q_1)}{\sqrt{p_1(1 - p_1)q_1(1 - q_1)}}, \quad (8)$$

$$S(\mathbf{x}, \mathbf{y}) = \frac{4(p_1 p_{11} - p_1 q_1) p_1 q_1}{(p_1 - p_1^2 + q_1 - q_1^2)(p_1^2 + q_1^2)}, \quad (9)$$

and

$$I(\mathbf{x}, \mathbf{y}) = h[p_{11}p_1 + (1 - p_{00})(1 - p_1)] + h[(1 - p_{11})p_1 + p_{00}(1 - p_1)] - (1 - p_1)[h(p_{00}) + h(1 - p_{00})] + p_1[h(p_{11}) + h(1 - p_{11})], \quad (10)$$

where the input binary image \mathbf{x} having two levels $\{x_0, x_1\}$ with $x_0 < x_1$, for which the probability to have a pixel with level x_1 is $\Pr\{x = x_1\} = p_1$ and $\Pr\{x = x_0\} = 1 - p_1$, the conditional probabilities $p_{1k} = \Pr\{y = 1|x = x_k\}$ and $q_1 = \Pr\{y = 1\} = p_1 p_{11} + (1 - p_1) p_{10}$ and function $h(u) = -u \log_2(u)$.

We are now ready to study the evolution of the similarity measures C, S , and I when the rms σ_n of the centered Gaussian white noise \mathbf{n} increases. As visible in Fig. 2, a non-monotonic evolution of the measures is observed. This is the signature of a stochastic resonance effect or nonlinear image transmission aided by noise. Optimal noise levels, maximizing the similarity measures, are observed in each case with C, S , and I . These optimal noise levels are close for the three measures and located around the noise level of Fig. 1(c) in accordance with the visual perception at $\sigma_{\text{opt}} \approx 0.5$.

We now consider the sequence of images of Figs. 1(e)–1(h). In Figs. 1(f)–1(h), and specifically in Fig. 1(g), the visual inspection does not perceive any noise aided image transmission, by contrast with Figs. 1(b)–1(d). However, in Figs. 1(e)–1(h), as in Figs. 1(a)–1(d), we deal with input images \mathbf{x} in (a) and in (e), which present the same proportion $p_1 = 0.84$ of white pixels. As a consequence, the quantitative pixel to pixel measures of similarity of Fig. 2 characterize the situation in Figs. 1(e)–1(h) as well as in Figs. 1(a)–1(d) since they are sensitive only to the first-order statistics of the images, as conveyed by p_i . On the basis of these measures of Fig. 2, a stochastic resonance effect equivalent in Figs. 1(e)–1(h) and in Figs. 1(a)–1(d) is predicted, while the visual perception in Figs. 1(e)–1(h) does not record any stochastic resonance effect. The visual perception in Figs. 1(a)–1(d) operates on single realizations of the noise \mathbf{n} in each successive image. This is by contrast with the quantitative measures of Fig. 2, which are ensemble averages over the noise \mathbf{n} . In the early study of stochastic resonance in visual perception [9], it was chosen to consider images with minimal structures (a frequency modulated sine) with a temporal variation of additive noise in images submitted to a group of human observers. The stochastic resonance effects recorded in [9] are obtained on average. Nonetheless, as shown in Figs. 1(a)–1(d), the nonlinear transmission aided by noise is perceivable by a human observer on a single realization, without the need to resort to ensemble averages over the noise as performed by the quantitative

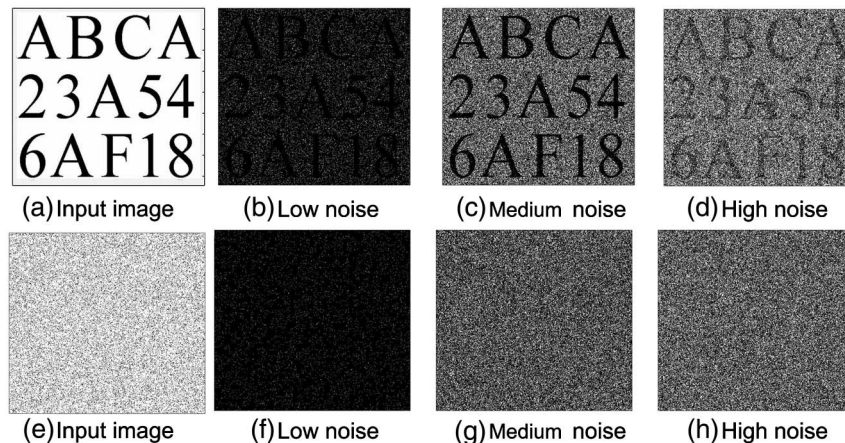


Fig. 1. (a) Initial binary input image \mathbf{x} with gray levels $x_0 = 0$ and $x_1 = 1$. (b)–(d) Binary images \mathbf{y} at the output of the two-level quantizer of Eqs. (1) and (2) with threshold $\theta = 1.1$, with the additive white noise \mathbf{n} taken centered with a Gaussian distribution with standard deviation $\sigma_n = 0.07$ (b), $\sigma_n = 0.49$ (c), and $\sigma_n = 1.5$ (d). (f)–(h) are identical to (b)–(d) with the input binary image (e) having the same proportions of black and white pixels as (a).

measures of Fig. 2. If the visual perception identifies a useful-noise effect in Figs. 1(a)–1(d) and not in Figs. 1(e)–1(f), it is probably by exploiting spatial structures present in the images of Figs. 1(a)–1(d) and absent in images of Figs. 1(e)–1(h). The consideration of the spatial structures in images therefore constitutes a new direction of investigation in the quantitative analysis of stochastic resonance, which we propose to initiate in the following sections.

3. INFLUENCE OF SPATIAL STRUCTURES IN IMAGES

The similarity measures used in Fig. 2 realize ensemble averages that give the same importance to each pixel and do not take into account salient regions in structured images. Such regions, salient in orientation or in gray-level contrast, are known [12] to fix the visual attention, i.e., to assign a greater informational importance to certain groups of pixels. In image processing, image structures are classically characterized with morphological attributes. Standard families of morphological attributes are contours, homogeneous regions, textures, and local features. Because they extract salient points in images, local features are good candidates to constitute measures of similarity inspired from the visual system, for objective study of the influence of spatial structures in the constructive action of the noise in imaging. A large variety of strategies for extraction of local features have been reported in the literature, from the early corner detectors up to the recent developments (see [13] for a recent review). Variations concern the invariance properties of these local features in terms of rotation, affine transformation, or scale. For illustration, in this article we use the scale invariant feature transform (SIFT), as originally introduced in [14], which we implement under the didactic soft version freely available at [15]. SIFT searches for keypoints, i.e., specific locations in space, corresponding to scale invariant extremas in the gradient of series of smoothed and resampled version of the original image. For each keypoint, a description vector is computed through measures achieved over the spatial neighborhood of the gradient. The keypoints and the associated description vectors can then be used to compare two images. SIFT searches for pairs of keypoints with similar description

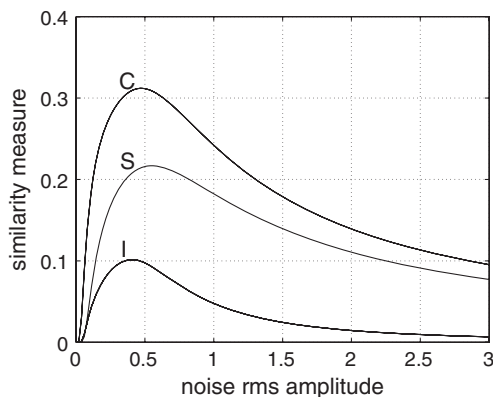


Fig. 2. Similarity measure between the input binary image x of Fig. 1(a) or Fig. 1(e) and the binary output image y as a function of the rms amplitude σ_n of the noise n taken zero-mean Gaussian. The normalized cross-covariance $C(x, y)$ of Eq. (3), the SSIM index $S(x, y)$ of Eq. (4), and the Shannon mutual information $I(x, y)$ of Eq. (5) are identical for Figs. 1(a) and 1(e).

vectors, which are called SIFT matches. The similarity measure is based on a simple scalar product of the two vectors. The higher the scalar product, the closer the local structures of the salient points. A threshold is then applied on these scalar products to decide if the local structures match or not. In this manuscript, we have used the default threshold setting given in [15]. (We have verified that the choice of this decision threshold does not affect the qualitative nonmonotonic SIFT matches evolution nor the value of the optimal noise level maximizing the number of SIFT matches in Fig. 3.) The description vector captures the local structure of salient points. Therefore, the number of SIFT matches between the input and output image stands as a good candidate for a measure of similarity, taking into account the spatial structures in images. Since the nonlinear image transmission we consider here in Eqs. (1) and (2) is a pixel to pixel transformation, we measure only the number of colocalized SIFT matches, i.e., SIFT matches corresponding to two keypoints in a pair with the same spatial localization in the output image y and the initial input image x . A demonstration of our SIFT matches counting procedure applied to images of Fig. 1 is given in Fig. 3. As visible in Fig. 3, when the level of the noise increases, a nonmonotonic evolution of the number of colocalized SIFT matches is obtained only for the input image Fig. 1(a) spatially structured. Meanwhile in Fig. 3, the number of colocalized SIFT matches identified in the nonstructured input image Fig. 1(e) remains at an artifactually low and quasi-constant level. This stochastic resonance signature is confirmed in Fig. 4, as the number of SIFT matches counted is plotted as a function of the noise rms amplitude.

For the input image Fig. 1(a) spatially structured, the measure of similarity of Fig. 4 based on SIFT is maximized for an optimal nonzero level of noise σ_{opt} . The stochastic resonance visually perceived in Fig. 1 is quantitatively assessed via SIFT, and moreover $\sigma_{\text{opt}} \approx 0.5$ remains unchanged and in accordance with the similarity measures C, S, I of Fig. 2. By contrast, for the input image Fig. 1(e) spatially unstructured, the measure of similarity based on SIFT remains at zero. This is also in accordance with the visual perception, while the similarity measures C, S, I failed to discriminate between structured and unstructured images having the same first-order statistics as Figs. 1(a) and 1(e). The comparison of Figs. 2 and 4 shows the relevance of our approach to account quantitatively and in terms of a psychovisual mechanism of local saliency, for the observable difference between Figs. 1(a)–1(d) and Figs. 1(e)–1(f).

4. INFLUENCE OF SPATIAL STRUCTURES IN NOISE

So far in this report, we have quantified with SIFT the influence of spatial structures in input image x on the visual perception of stochastic resonance. Noise can also carry spurious spatial structures. And it would be interesting to study the influence of those spurious spatial structures on the visual perception of stochastic resonance. A noise that is naturally found with spurious spatial structures is the speckle noise appearing in coherent imaging. The speckle noise, generated by the irregularities of the scene at the wavelength scale, is not white noise but colored noise with strong spatial correlation over the speckle grain size [16]. In the following, we propose to study the influence of the size of the speckle grain on the visual perception of the stochastic resonance.

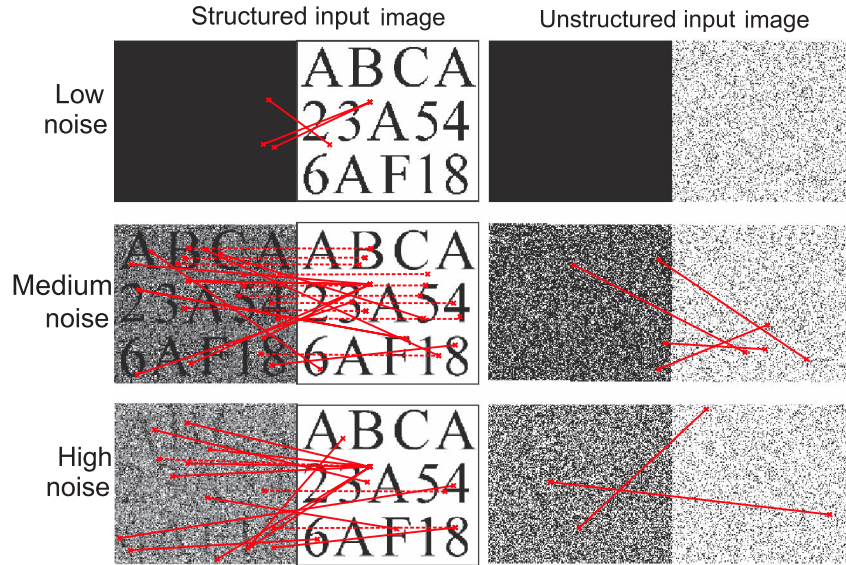


Fig. 3. (Color online) Input–output similarity based on the number of colocalized SIFT matches counted in the images of Fig. 1. Lines materialize the keypoints detected as matching in the input and in the output image. Dashed horizontal lines are for colocalized SIFT matches associating pairs of keypoints with same spatial location in input and output images. Solid lines, mainly oblique, are for SIFT matches with wrong locations. The left column corresponds to the structured image of Fig. 1(a), and the right column to the unstructured image of Fig. 1(e).

Let the speckle noise \mathbf{n} take the form of fully developed speckle, which is commonly modeled [16] as a multiplicative noise, with first-order statistics given by an exponential probability density $p_n(j)$

$$p_n(j) = \frac{1}{\sigma_n} \exp\left(-\frac{j}{\sigma_n}\right), \quad j \geq 0 \quad (11)$$

with mean and standard deviation σ_n and rms amplitude $\sqrt{2}\sigma_n$. The conditional probability p_{1k} amounts to $\Pr\{n > \theta/x_k\} = 1 - F_n(\theta/x_k)$, with $k \in \{0, 1\}$, where $F_n(j) = \int_{-\infty}^j p_n(j') dj'$ is the cumulative distribution of the noise \mathbf{n} . When the probability density $p_n(j)$ of the speckle noise is given by Eq. (11), we have

$$F_n(j) = 1 - \exp\left(-\frac{j}{\sigma_n}\right), \quad j \geq 0. \quad (12)$$

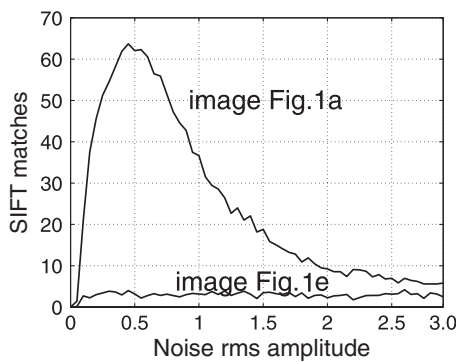


Fig. 4. Average number of colocalized SIFT matches found over 100 realizations between initial input binary images \mathbf{x} [Fig. 1(a) or Fig. 1(e)] and the output binary image \mathbf{y} , as a function of the noise level. By contrast with the similarity measures of Fig. 2, the number of colocalized SIFT matches differs for the structured image of Fig. 1(a) and the unstructured image Fig. 1(e), for which the number of colocalized SIFT matches detected is artifactually low and constant.

We then consider the same input–output image transmission scheme with a binary image \mathbf{x} corrupted with the multiplicative speckle noise \mathbf{n}

$$\mathbf{y} = g(\mathbf{x} \times \mathbf{n}), \quad (13)$$

and transmitted by the same two-level quantizer with threshold θ of Eq. (2). Equations (3)–(5) expressed for binary input images and binary output similarity measures C, S, I remain valid with only the p_{1k} , which depends on the signal-noise coupling. As illustrated in Fig. 5, the stochastic resonance effect is predicted by the pixel-based similarity measure with multiplicative speckle noise coupling. This has been first shown in [7,8]. It appears from [7,8] that stochastic resonance with multiplicative speckle noise is recorded also by human visual perception and in good accordance with pixel-based similarity measures C, S, I as long as the speckle grain is small in

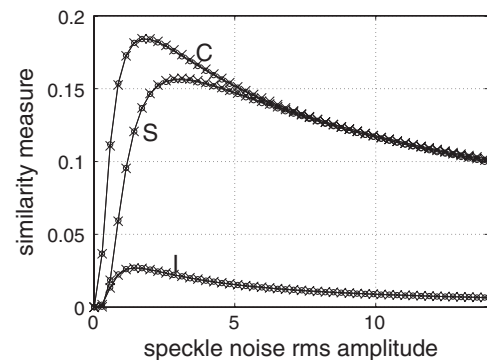


Fig. 5. Same input binary images as in Fig. 1 with gray levels $x_0 = 0.5, x_1 = 1$ and threshold $\theta = 1$. The multiplicative speckle noise \mathbf{n} is exponentially distributed as in Eq. (11) with rms amplitude $\sqrt{2}\sigma_n$. Solid lines stand for the normalized cross-covariance $C(\mathbf{x}, \mathbf{y})$ of Eq. (3), and the SSIM index $S(\mathbf{x}, \mathbf{y})$ of Eq. (4) and the Shannon mutual information $I(\mathbf{x}, \mathbf{y})$ of Eq. (5) are identical for Figs. 1(a) and 1(e). The discrete set of points stands for the numerical average over 100 realizations with the speckle grain size of Fig. 6(b)—circles and Fig. 6(d)—crosses.

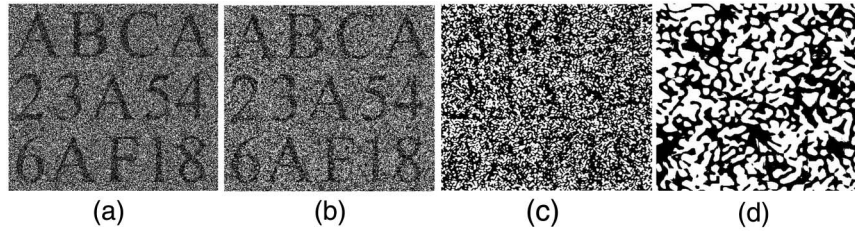


Fig. 6. Output images with the same speckle noise rms amplitude taken at $\sqrt{2}\sigma_n = 1.5$. Input image is the binary image of Fig. 1(a) with gray levels $x_0 = 0.5$, $x_1 = 1$, threshold $\theta = 1$. From left to right, the size of the speckle grain is increased.

comparison to the informative structures carried by the input image.

In simulation, the spatial correlation of the speckle noise can be controlled by choosing the number of random phasors, representing the number of irregularities at the wavelength scale, used to generate the speckle pattern (see [16] for detailed procedure). A small number of random phasors result in a spatially colored speckle noise with large grains, while a large number of random phasors produces an almost white speckle noise. Choosing the number of random phasors only affects the second-order statistics, while the gray level remains exponentially distributed as in Eq. (11). Consequently, the size of the speckle grain has no influence on the first-order statistics-based similarity measures C , S , and I , as numerically demonstrated in Fig. 5 with an almost perfect agreement between theory and numerical simulation with various speckle grain size. In Fig. 6, we provide, for the same input binary image, output binary images with a fixed speckle noise level while increasing the size of the speckle grain. As perceivable in Fig. 6, our visual capability to extract the informative structures carried by the input binary image in the output binary image is strongly affected by the apparition of the spurious structures carried by the speckle noise. This is especially the case when the speckle grain size increases up to the point where it becomes of size similar to the informative structures as in Fig. 6(d). Yet, since the first-order statistics of images of Fig. 6 are identical, the pixel-based measures C , S , I fail to record the impact of the spurious structures of speckle on the visual perception of the stochastic resonance effect.

This is by contrast with the colocalized SIFT matches of the previous section, which show in Fig. 7 in good agreement with the visual perception. In Fig. 7, the nonmonotonic evolution of

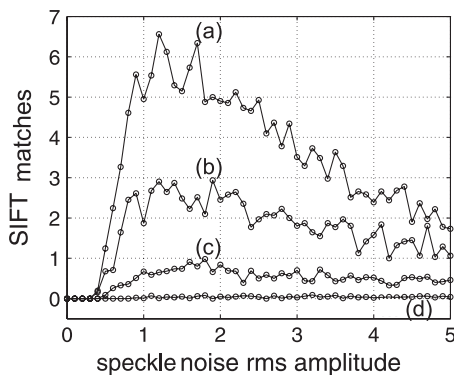


Fig. 7. Average number of colocalized SIFT matches found over 100 realizations between the initial input binary image x [Fig. 1(a)] and the output binary image y , as a function of the speckle noise level. Gray levels $x_0 = 0.5$, $x_1 = 1$, threshold $\theta = 1$. Plots (a), (b), (c), and (d) are obtained with grain sizes increasing for the speckle as in Fig. 6.

the number of colocalized SIFT matches as a function of the speckle noise level is preserved for not-too-large speckle grain size. The optimal level of noise in the stochastic resonance effect is not affected, and only the peak is reduced when the speckle grain size is raised. This again demonstrates the interest of our local-feature-based similarity measure to assess stochastic resonance in visual perception of spatially structured images.

5. CONCLUSION AND PERSPECTIVES

We have demonstrated that pixel-based measures from first-order statistics are not sufficient to assess the visual perception of stochastic resonance. We have then introduced a higher-order new measure based on spatially colocalized SIFT to take into account the spatial structures in images. We have demonstrated the ability of this measure to quantify the influence of the structures of the information carrying images and the influence of a grainy speckle noise in the visual perception of the stochastic resonance with coherent imaging. This approach opens multiple perspectives for further investigation.

There exist many other measures modeling various aspect of the human psychovisual system, and it would be interesting to test their ability to respond in accordance with the human perception of stochastic resonance. Psychovisual saliency maps [12] modeling visual attention could be, for instance, an interesting candidate. Also, at the level of the eye itself, the effect of stochastic resonance has been studied experimentally and in numerical simulations at time scales of microseconds where microtremors of the gaze on the retina can be acquired. Stochastic resonance has also been shown in response to visual stimuli of a duration of 1/10 second [17]. Intermediate time scales could also be investigated by using eye tracking systems that follow the fixations of the eye at time scale of milliseconds [18]. A specific informational task would have to be defined to allow a quantification. One could think of following the edge of an object, for instance. The perceived statistical properties of the images are expected to be also impacted by the observation scale of images on the visual perception of stochastic resonance would therefore be another possible direction of investigation. Finally, for unstructured images, as demonstrated by our work, first-order statistics-based similarity measures fail to report the absence of perceived stochastic resonance. The quantification of the frontier between a structured and an unstructured image with regard to stochastic resonance is now an open question. Considerations at the pixel level quantifying the compressibility or sparsity, as in compressive sensing [20] of the input image, could constitute a direction. At the spatial frequency level, considerations could also be made to quantify the presence or absence of structures characterized

by the statistical power-law signature of natural images in the Fourier domain [21]. More elaborate measures at the semantic level could quantify the amount of “memorability” of the structures in the input image [22] proposed for visual perception in stochastic resonance experiments.

REFERENCES

1. M. D. McDonnell, N. G. Stocks, C. E. M. Pearce, and D. Abbott, *Stochastic Resonance: From Suprathreshold Stochastic Resonance to Stochastic Signal Quantization* (Cambridge University, 2008).
2. B. M. Jost and B. E. A. Saleh, “Signal-to-noise ratio improvement by stochastic resonance in a unidirectional photorefractive ring resonator,” *Opt. Lett.* **21**, 287–289 (1996).
3. F. Vaudelle, J. Gazengel, G. Rivoire, X. Godivier, and F. Chapeau-Blondeau, “Stochastic resonance and noise-enhanced transmission of spatial signals in optics: the case of scattering,” *J. Opt. Soc. Am. B* **15**, 2674–2680 (1998).
4. K. P. Singh, G. Ropars, M. Brunel, and A. Le Floch, “Stochastic resonance in an optical two-order parameter vectorial system,” *Phys. Rev. Lett.* **87**, 213901 (2001).
5. F. Marino, M. Giudici, S. Barland, and S. Balle, “Experimental evidence of stochastic resonance in an excitable optical system,” *Phys. Rev. Lett.* **88**, 040601 (2002).
6. D. V. Dylov and J. W. Fleischer, “Nonlinear self-filtering of noisy images via dynamical stochastic resonance,” *Nat. Photon.* **4**, 323–328 (2010).
7. S. Blanchard, D. Rousseau, D. Gindre, and F. Chapeau-Blondeau, “Constructive action of the speckle noise in a coherent imaging system,” *Opt. Lett.* **32**, 1983–1985 (2007).
8. F. Chapeau-Blondeau, D. Rousseau, S. Blanchard, and D. Gindre, “Optimizing the speckle noise for maximum efficacy of data acquisition in coherent imaging,” *J. Opt. Soc. Am. A* **25**, 1287–1292 (2008).
9. E. Simonotto, M. Riani, C. Seife, M. Roberts, J. Twitty, and F. Moss, “Visual perception of stochastic resonance,” *Phys. Rev. Lett.* **78**, 1186–1189 (1997).
10. D. Rousseau, A. Delahaies, and F. Chapeau-Blondeau, “Structural similarity measure to assess improvement by noise in nonlinear image transmission,” *IEEE Signal Process. Lett.* **17**, 36–39 (2010).
11. Z. Wang and A. C. Bovik, “A universal image quality index,” *IEEE Signal Process. Lett.* **9**, 81–84 (2002).
12. L. Itti, C. Koch, and E. Niebur, “A model of saliency-based visual attention for rapid scene analysis,” *IEEE Trans. Pattern Anal. Machine Intell.* **20**, 1254–1259 (1998).
13. J. Li and N. M. Allison, “A comprehensive review of current local features for computer vision,” *Neurocomputing* **71**, 1771–1787 (2008).
14. D. G. Lowe, “Distinctive image features from scale-invariant keypoints,” *Int. J. Comput. Vis.* **60**, 91–110 (2004).
15. <http://www.vlfeat.org/~vedaldi/code/sift.html>.
16. J. W. Goodman, *Speckle Phenomena in Optics: Theory and Applications* (Roberts & Company, 2006).
17. F. Moss, L. M. Ward, and W. G. Sannita, “Stochastic resonance and sensory information processing: a tutorial and review of application,” *Clin. Neurophysiol.* **115**, 267–281 (2004).
18. A. T. Duchowski, *Eye Tracking Methodology: Theory and Practice* (Springer, 2007).
19. A. Delahaies, D. Rousseau, and F. Chapeau-Blondeau, “Joint acquisition-processing approach to optimize observation scales in noisy imaging,” *Opt. Lett.* **36**, 972–974 (2011).
20. A. Delahaies, D. Rousseau, D. Gindre, and F. Chapeau-Blondeau, “Exploiting the speckle noise for compressive sensing,” *Opt. Commun.* **284**, 3939–3945 (2011).
21. D. Ruderman and W. Bialek, “Statistics of natural images: scaling in the woods,” *Phys. Rev. Lett.* **73**, 814–817 (1994).
22. P. Isola, J. Xiao, A. Torralba, and A. Oliva, “What makes an image memorable?” in *Proceedings of IEEE Conference on Computer Vision and Pattern Recognition* (IEEE, 2011), pp. 145–156.